Redox processes in $Li_xNi_{1-y}Co_yO_2$ cobalt-rich phases

Ismael Saadoune, Michel Ménétrier and Claude Delmas*

Institut de Chimie de la Matière Condensée de Bordeaux-CNRS and Ecole Nationale Supérieure de Chimie et Physique de Bordeaux, Av. Dr A. Schweitzer, 33608 Pessac cedex, France

Samples of $Li_xNi_{0.1}Co_{0.9}O_2$ ($0.5 \leqslant x \leqslant 1.0$), prepared by electrochemical deintercalation from $LiNi_{0.1}Co_{0.9}O_2$, have been characterized by X-ray diffraction, electrical measurements and ^{7}Li NMR spectroscopy. A good correlation is found between the electrochemical behaviour of the $Li_xNi_{0.1}Co_{0.9}O_2$ electrode materials and their physical properties. During lithium deintercalation from $LiNi_{0.1}Co_{0.9}O_2$, the trivalent nickel ions are oxidized preferentially to trivalent cobalt ions. This leads to a reversible break in the potential–composition curve around the composition $Li_{0.9}Ni_{0.1}Co_{0.9}O_2$. This change in the redox regime, which occurs without any structural transformation, has been confirmed by the evolution of the electrical conduction process and that of the ^{7}Li NMR signal.

Since the discovery of the ability of some varieties of carbon to intercalate lithium reversibly, many studies have been carried out on the preparation and characterization of very oxidizing lithiated oxides able to be used as positive electrode in 'lithium-ion' batteries. Among all investigated materials, $LiCoO_2$, $LiNiO_2$, $LiNi_{1-y}Co_yO_2$ and $LiMn_2O_4$ are the most interesting.[1–11]

For the mixed $LiNi_{1-y}Co_yO_2$ system, previous surveys have shown that this solid solution exhibits very interesting electrochemical properties which allow construction of realistic commercial batteries.[12] From a structural point of view, all these materials crystallise in the rhombohedral system (space group $R\bar{3}m$) with the layered α-$NaFeO_2$ type structure. Moreover, for low cobalt content ($y < 0.2$), a detailed structural characterization has demonstrated the occurrence of a small departure from stoichiometry.[13] Indeed, a few divalent nickel ions occupy the lithium planes. During deintercalation, their oxidation to the trivalent state leads to a local collapse of the interslab spaces, and therefore limits the lithium reintercalation at the next discharge.[14] For larger cobalt amounts ($y \geqslant 0.2$), the structure becomes strictly two-dimensional and therefore these materials exhibit a good reversibility upon reintercalation. Note that these lamellar oxides, prepared at high temperature, are often referred to as HT-$LiNi_{1-y}Co_yO_2$ in contrast with LT-$LiNi_{1-y}Co_yO_2$ prepared at 400 °C, which has different structure and electrochemical properties.[15,16]

We have recently studied the changes of structural and physical properties with the lithium amount in the $Li_xNi_{0.8}Co_{0.2}O_2$ nickel rich phase.[17] We have shown that Ni^{4+}/Ni^{3+} is the only couple which participates in the redox process during lithium deintercalation in the range $0.4 \leqslant x \leqslant 1.0$. The aim of the present work is to describe the results of electrochemical, structural and physical studies of $Li_xNi_{0.1}Co_{0.9}O_2$ ($0.5 \leqslant x \leqslant 1.0$) cobalt rich phases in which both the Ni^{4+}/Ni^{3+} and Co^{4+}/Co^{3+} redox couples must be involved during lithium deintercalation. ^{7}Li NMR on $LiNi_{1-y}Co_yO_2$ materials[18] has shown a very strong sensitivity to the presence of unpaired electrons from Ni^{3+}, whereas Co^{3+} is indeed diamagnetic. Therefore, one can expect to be able to discriminate between the possible oxidation of (paramagnetic) Ni^{3+} to (diamagnetic) Ni^{4+} and that of (diamagnetic) Co^{3+} to (paramagnetic) Co^{4+} on the basis of ^{7}Li NMR spectroscopy.

Experimental

The $LiNi_{0.1}Co_{0.9}O_2$ oxide was prepared, as described in ref. 12, by the calcination of a pelletized mixture of NiO, Co_3O_4 and Li_2CO_3 at 500 °C for 24 h under dry oxygen, followed by a heat treatment at 900 °C for 24 h with grinding. After reaction, the sample was allowed to cool slowly to room temperature.

Electrochemical studies were carried out using Li/$LiClO_4$ in propylene carbonate/$Li_xNi_{0.9}Co_{0.1}O_2$ cells. For classical electrochemical experiments, the positive electrode (*ca.* 10 mA h cm^{-2}) was constituted of a mixture of 90% by mass of active material and 10% of ketjenblack, with no binder. In the case of the electrochemical preparation of partially deintercalated phases for physical characterization, the pure $LiNi_{0.1}Co_{0.9}O_2$ phase was used without carbon as electronic conductor; the capacity of the electrode was then *ca.* 20 mA h cm^{-2}. In the case of materials prepared for the electronic properties study, sintered pellets (3 tonnes for a 0.8 cm diameter, followed by a thermal treatment of 12 h at 800 °C under oxygen) of the starting phase were used as positive electrode. The 1.5 mm thick pellets obtained in such conditions exhibit a compactness close to 80% The cells, assembled in an argon-filled dry box, were charged at a very low current density (70 μA cm^{-2}). For the thermodynamic potential measurements (open circuit voltage), the charge process was interrupted by relaxation periods. In order to be as close as possible to the equilibrium conditions, the relaxation periods were interrupted when the slope of the voltage–time curve was smaller than 0.1 mV h^{-1}.

In fact, lithium deintercalation from $LiNi_{0.1}Co_{0.9}O_2$ could also be realized chemically by using the very strong oxidizing agent NO_2BF_4 in CH_3CN. Nevertheless, this chemical method, even if realized under optimal conditions, may lead to inhomogeneity in the resulting phase and therefore it is quite difficult to obtain the desired composition in a reproducible way. The physical properties of the chemically oxidized materials may then be very different from those of the materials obtained electrochemically.

Powder diffraction data were collected on an 'INEL curve position-sensitive detector' using Co-Kα radiation. In order to avoid possible contamination, experiments were performed in sealed capillaries (under dry argon). For the electrical conductivity measurements, a four-probe method was used with direct current. The thermoelectronic measurements have been carried out by using equipment described elsewhere.[19] ^{7}Li NMR spectra of $Li_xNi_{0.1}Co_{0.9}O_2$ ($0.7 \leqslant x \leqslant 1.0$) phases were obtained using an FT Bruker MSL 200 spectrometer at 77.7 MHz. All spectra, measured with a static echo type sequence [$\pi/2$ pulse (3.8 μs); 20 μs delay; $\pi/2$ pulse], are referred to a 1 M LiCl solution (δ 0).

Results and Discussion

The X-ray diffraction pattern of HT-$LiNi_{0.1}Co_{0.9}O_2$, shown in Fig. 1, is characteristic of a single phase with an α-$NaFeO_2$

† Present addres: Université Cadi Ayyad, FST Marrakech, BP 618, Marrakech, Maroc.

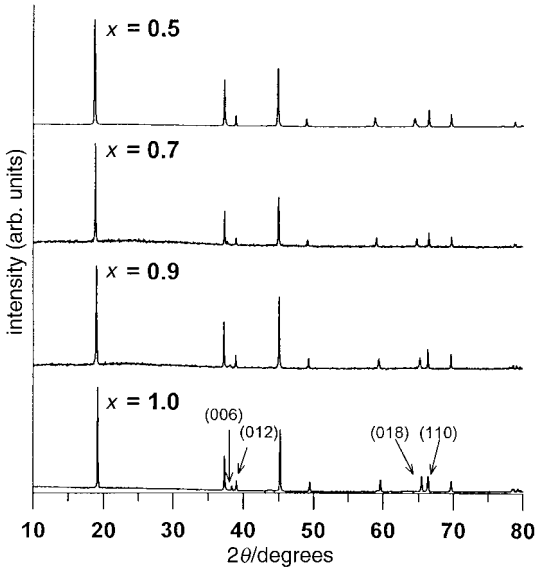

Fig. 1 X-Ray diffraction patterns of the $Li_xNi_{0.1}Co_{0.9}O_2$ phases ($0.5 \leqslant x \leqslant 1$)

type structure. Lithium ions are in octahedral sites between $(Ni_{0.1}Co_{0.9}O_2)_n$ infinite slabs formed by edge-sharing $(Ni_{0.1}Co_{0.9})O_6$ octahedra. Hexagonal cell parameters, obtained by least-squares refinement, $a = 2.818$ and $c = 14.06$ Å, are different from those of LT-$LiNi_{0.1}Co_{0.9}O_2$ ($a = 2.833$, $c = 13.881$ Å) in which the cationic distribution is disordered.[15] For the former oxide, a c/a ratio very different from the critical $2\sqrt{6}$ value and a clear splitting of the (006) and (012) as well as (018) and (110) diffraction lines indicate an ordered distribution of the lithium and transition-metal ions in the structure.

Electrochemical study

Fig. 2 shows the first charge and discharge curves of an $Li//Li_xNi_{0.1}Co_{0.9}O_2$ electrochemical cell ($J = 150$ μA cm^{-2}). This cycling curve exhibits two flat domains separated by a potential jump from 3.6 to 3.9 V around the $Li_{0.9}Ni_{0.1}Co_{0.9}O_2$ composition during the charge process. In order to achieve a better characterization of the thermodynamics of this system, an OCV charge curve has been plotted (Fig. 3). This curve shows that in the flat domains, the potential increases continuously, which suggests the occurrence of a monophasic reaction throughout the cycling. The potential jump occurs when 0.1 mol lithium ions are deintercalated, which corresponds to the nickel content of the mixed oxide. At the beginning of the deintercalation process the charge curve is similar to that of an $Li//Li_xNiO_2$ cell, while for $x < 0.9$, the charge curve becomes

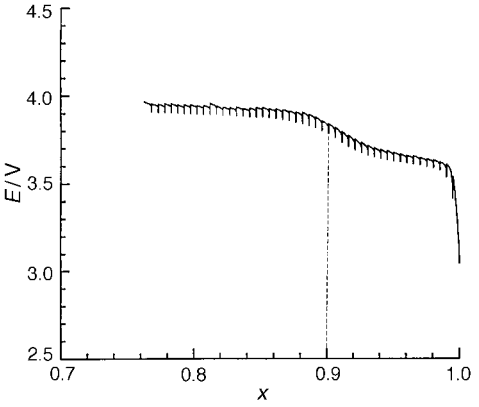

Fig. 3 First intermittent charge–relaxation curve of an $Li//Li_xNi_{0.1}Co_{0.9}O_2$ cell. ($J = 70$ μA cm^{-2}; relaxation criterion: $\Delta E/\Delta t = 0.1$ mV h^{-1}).

close to that of $Li//Li_xCoO_2$. As discussed further, this evolution agrees with the result obtained in the nickel-rich $Li_xNi_{0.8}Co_{0.2}O_2$ system, which suggests that Ni^{3+} ions are oxidized preferentially to Co^{3+}.[17] It should be noted that the fully intercalated phase is difficult to restore during discharge (intercalation reaction). This could be probably attributed to a kinetics problem especially as the $Li_xNi_{0.1}Co_{0.9}O_2$ phase becomes close to electronically insulating at $x \approx 1$. This point will be discussed further.

The reversible crossover between the two different redox processes is confirmed by a similar electrochemical study of an $Li//Li_xNi_{0.2}Co_{0.8}O_2$ cell. Fig. 4 shows the shape of the charge curves for $Li//Li_xNi_{1-y}Co_yO_2$ ($y = 0.8$, 0.9, 1.0) cells. Note that the electrochemical behaviour of the $LiCoO_2$ electrode is identical to those published by several authors;[1,20] the potential range scanned during the deintercalation reaction from $LiCoO_2$ (oxidation process) reflects the strong oxidizing power of Co^{4+} ions. As detected in the case of $Li_xNi_{0.1}Co_{0.9}O_2$ phases, a break in the potential–composition curve of the $Li//Li_xNi_{0.2}Co_{0.8}O_2$ electrochemical cell is evidenced, but around $x = 0.8$ *cf.* $x = 0.9$ for the former case. This again indicates a change in the electrochemical regime upon lithium deintercalation.

X-Ray diffraction study

One may wonder whether any structural modification accompanies this break in the $Li//Li_xNi_{0.1}Co_{0.9}O_2$ potential–composition curve. In order to study this, the X-ray diffraction patterns for $Li_xNi_{0.1}Co_{0.9}O_2$ phases were recorded after electrochemical deintercalation of lithium using a charge process. Fig. 1 shows the diffraction patterns of $Li_xNi_{0.1}Co_{0.9}O_2$ ($x = 1$,

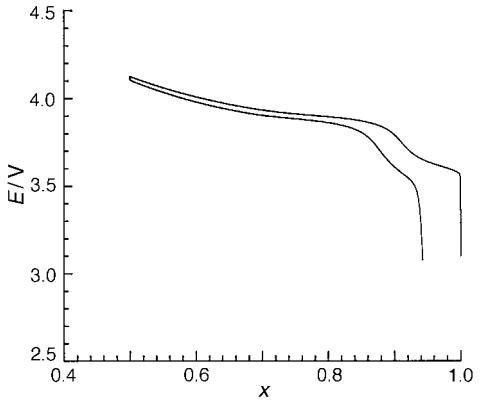

Fig. 2 First galvanostatic charge–discharge cycle of an $Li//Li_xNi_{0.1}Co_{0.9}O_2$ electrochemical cell ($J = 150$ μA cm^{-2})

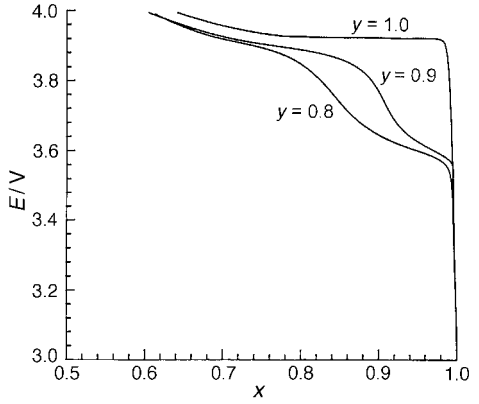

Fig. 4 Charge curves of $Li//Li_xNi_{1-y}Co_yO_2$ cells for various amounts of cobalt ($0.8 \leqslant y \leqslant 1$) ($J = 70$ μA cm^{-2})

0.9, 0.7, 0.5). All materials exhibit sharp peaks indicating the maintenance of a good crystallinity throughout the electrochemical deintercalation. This indicates that the host framework remains stable during cycling in accordance with the topotactic character of such an intercalation/deintercalation reaction. All the X-ray patterns can be easily indexed in the hexagonal system (α-$NaFeO_2$ type structure) without any evidence of peaks corresponding to the monoclinic phase as was observed for the Li_xNiO_2[21] and Li_xCoO_2[22] systems. Furthermore, the splitting between the (018) and (110) diffraction peaks shows a continuous cell parameter variation upon deintercalation. This confirms that the jump in potential of the $Li//Li_xNi_{1-y}Co_yO_2$ ($y=0.8$, 0.9) cells must be due only to an electronic phenomenon.

Fig. 5 shows the variation of the hexagonal cell parameters of $Li_xNi_{0.1}Co_{0.9}O_2$ phases ($0.5 \leqslant x \leqslant 1.0$). Lithium extraction from $LiNi_{0.1}Co_{0.9}O_2$ induces simultaneously an expansion of the interslab distance (c_{hex} cell parameter) and a small decrease of the metal–metal intrasheet distance (a_{hex} cell parameter).

These evolutions are similar to those of most A_xMO_2 lamellar oxides.[21–23] The increase of the interslab distance is caused by the strengthening of the repulsive interaction between the oxygen atoms of adjacent layers after deintercalation. On the other hand, the metal–metal intrasheet distance decreases in the composition range $0.7 \leqslant x \leqslant 1.0$ as x decreases. This decrease is due to the appearance of Ni^{4+} and Co^{4+} which have smaller ionic radii than Ni^{3+} and Co^{3+}. Nevertheless, for $x<0.7$, the a parameter remains almost constant and equal to 2.805 Å. This value reflects the compactness of the oxygen packing within the $(Ni_{0.1}Co_{0.9}O_2)_n$ slabs ($R_{O^{2-}}=1.40$ Å).[24]

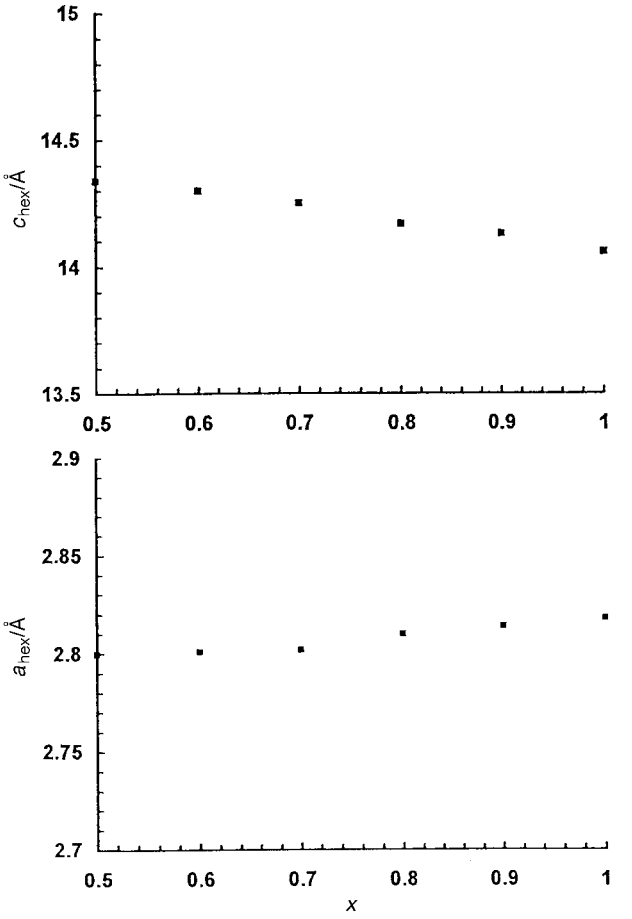

Fig. 5 Hexagonal cell parameters of the $Li_xNi_{0.1}Co_{0.9}O_2$ phases ($0.5 \leqslant x \leqslant 1$)

Electronic properties study

Electrical conductivity. As the break in the $Li//Li_xNi_{0.1}Co_{0.9}O_2$ electrochemical curve is believed to have only an electronic origin, a systematic study of the evolution of the electronic transport properties for various $Li_xNi_{0.1}Co_{0.9}O_2$ phases has been performed. Fig. 6 shows the variation of the electronic conductivity *vs.* reciprocal temperature for compositions corresponding to $x=1$, 0.95, 0.9, 0.8, 0.7 and 0.6.

In the $LiNi_{0.1}Co_{0.9}O_2$ oxide, trivalent nickel and cobalt ions adopt a low-spin configuration.[9] Therefore, Co^{3+} ions are diamagnetic ($t_2^6e^0$) and only Ni^{3+} ions participate in the conduction process. The insulator character of this starting phase is due to the very small amount of active Ni^{3+} ions and to the absence of Ni^{4+}.

Under the hypothesis of a preferential oxidation of Ni^{3+} ions, the $Li_xNi_{0.1}Co_{0.9}O_2$ phases must contain Ni^{3+}, Ni^{4+} and Co^{3+} ions for $0.9<x<1.0$. The conduction phenomenon, which results from a $Ni^{3+}-O-Ni^{4+}$ hopping, remains thermally actived showing an electronic localization in these phases. The increase in electronic conductivity (Table 1) is due to the increase of Ni^{4+} ion concentration which favours electronic hopping. The difference in activation energy emphasizes that the transport mechanisms are different for the two phases ($x=1.0$, 0.95). For $LiNi_{0.1}Co_{0.9}O_2$, all nickel ions are trivalent, while for $Li_{0.95}Ni_{0.1}Co_{0.9}O_2$, 50% are trivalent and 50% are tetravalent. Nevertheless, the conductivity remains very low in comparison to the values obtained for the homologous nickel-rich $Li_{0.9}Ni_{0.8}Co_{0.2}O_2$ phase.[17] It should be noted that as the nickel amount is very low, most NiO_6 octahedra are isolated and therefore do not share any oxygen atoms with other NiO_6 octahedra. In this case, the hopping is considerably hindered.

For the $Li_{0.9}Ni_{0.1}Co_{0.9}O_2$ composition, the selective oxidation model previously proposed should lead to a material with a very low conductivity since all ions are in a diamagnetic state. In fact, the conductivity of $Li_{0.9}Ni_{0.1}Co_{0.9}O_2$ is higher than that of $Li_{0.95}Ni_{0.1}Co_{0.9}O_2$. Therefore, one can suspect that cobalt oxidation must occur before the complete oxidation

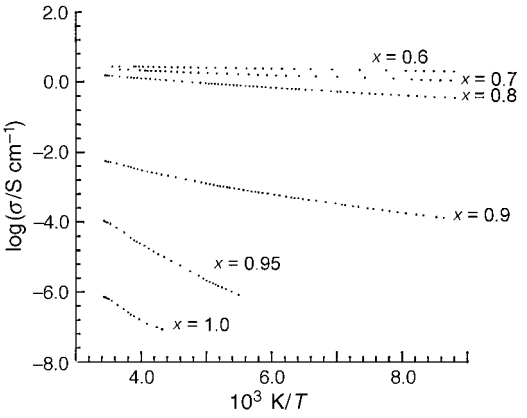

Fig. 6 Variation of the electronic conductivity *versus* reciprocal temperature for $Li_xNi_{0.1}Co_{0.9}O_2$ phases ($0.6 \leqslant x \leqslant 1$)

Table 1 Variation of the activation energy and electronic conductivity (at 25 °C) with lithium amount x in the $Li_xNi_{0.1}Co_{0.9}O_2$ phases

x	ΔE_a/eV	$\log[\sigma_{25\,°C}/\Omega^{-1}\,cm^{-1}]$
1.0	0.23	−6.2
0.95	0.13	−4.1
0.9	0.07	−2.4
0.8	0.03	0.2
0.7	0.02	0.4
0.6	0.01	0.5

of trivalent nickel ions. This point will be discussed further in detail.

As seen in Table 1, the electrical conductivity of the $Li_xNi_{0.1}Co_{0.9}O_2$ ($x<0.9$) bronzes exhibits high values but nevertheless still presents a thermally activated character, though the activation energy is considerably lower. The increase of the conductivity in this composition range arises from the appearance of Co^{4+} ions with incompletely filled t_2 orbitals. This leads to t_2–t_2 orbital overlapping through shared octahedra edges. As the Co^{4+}–Co^{4+} distance is smaller than the critical one, given by Goodenough's formula[25] ($R_c=2.89$ Å), a metallic behaviour should be expected, as observed for the Li_xCoO_2 system.[26] Nevertheless, the presence of Ni ions in the slab, and a statistical Li^+ distribution in the interslab space coupled to the anisotropic structural character of these lamellar oxides would lead to an electronic behaviour different from that of a classical metal. Besides, one must keep in mind that the conductivity experiments were carried out on sintered pellets which were electrochemically deintercalated. It is a possibility that the cell parameter modifications resulting from the deintercalation process can lead to grain boundary problems which introduce a parasitic activation energy.

Thermoelectronic power measurements. The thermal variation of the thermoelectronic power for the $Li_xNi_{0.1}Co_{0.9}O_2$ ($x=0.9$, 0.8, 0.7, 0.6) phases is shown in Fig. 7. The insulator character of the pristine $LiNi_{0.1}Co_{0.9}O_2$ phase makes measurement of thermoelectronic properties difficult. In all cases ($x\leqslant0.9$), the Seebeck coefficient has positive values indicating that electron holes are the main charge carriers in the conduction mechanism, in good agreement with an oxidation of trivalent cobalt ions which creates electron holes in the t_2 energy band. During lithium deintercalation, the Seebeck coefficient value decreases as a result of the increasing number of charge carriers in this cobalt band. Furthermore, the quasi-linearity of the $\alpha=f(T)$ plots and the relatively low absolute values of the Seebeck coefficient of the very deintercalated phases ($x<0.8$) are typical of a metallic behaviour. Nevertheless, as shown by the electronic conductivity measurements, even though these phases are good electronic conductors, a very small activation remains showing a rather complex behaviour.

For the $Li_{0.9}Ni_{0.1}Co_{0.9}O_2$ composition, the thermoelectronic power coefficient *vs.* temperature curve seems to fit with the continuous change observed for the more deintercalated phases, whereas a completely different behaviour would be observed if all ions were in a diamagnetic state. This behaviour, which is related to that observed for the conductivity measurements, shows that the cobalt oxidation must begin before the complete oxidation of the nickel ions. This point will be discussed with more detail in the general discussion.

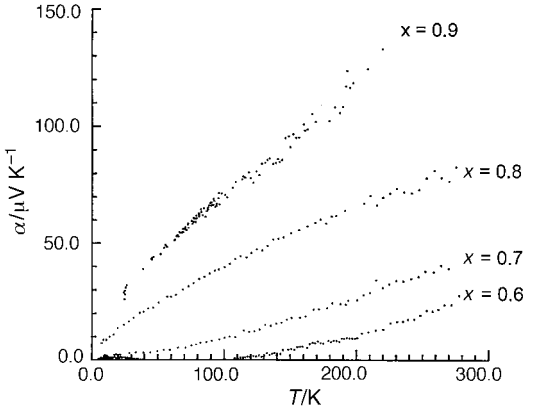

Fig. 7 Thermal variation of the Seebeck coefficient of the $Li_xNi_{0.1}Co_{0.9}O_2$ phases ($0.6\leqslant x\leqslant0.9$)

From these electronic transport results and those of the $Li_xNi_{0.8}Co_{0.2}O_2$ nickel-rich phases, a simplified energy diagram is proposed in Fig. 8. The above transport properties suggest a small polaron type behaviour at low deintercalation amounts, for which the electronic transport results from the nickel oxidation. On the contrary, a metallic-type conductivity appears when cobalt oxidation has occurred. Therefore, when small polaron conductivity occurs, one can assume the existence of narrow bands associated with $M^{n+}/M^{(n-1)+}$ redox couples, while when metallic conductivity occurs, one must consider the broad t_2 band resulting from the direct overlapping of the t_2 orbitals *via* common edges of the octahedra.

The preferential oxidation of Ni^{3+} ions compared to Co^{3+} ones leads one to consider that the energy of the Ni^{4+}/Ni^{3+} redox couple is higher than that of the t_2 (Co) band. As confirmed by a previous study concerning some hydroxides,[27] Co^{2+} ions are more reducing than Ni^{2+}. This rationalizes the higher energy of the Co^{3+}/Co^{2+} redox couple in comparison to the Ni^{3+}/Ni^{2+} couple. Note that these two bands are empty in the $LiNi_{0.1}Co_{0.9}O_2$ starting material whereas the Ni^{4+}/Ni^{3+} and t_2 (Co) bands are filled.

During lithium deintercalation from $LiNi_{0.1}Co_{0.9}O_2$, the Fermi level moves from the top to the bottom of the Ni^{4+}/Ni^{3+} band for $0.9\leqslant x\leqslant1.0$. In this composition range, the electronic conduction mechanism in the $Li_xNi_{0.1}Co_{0.9}O_2$ phases occurs *via* a $Ni^{4+}-O-Ni^{3+}$ hopping (small polaron). For $x<0.9$, lithium deintercalation leads to the oxidation of Co^{3+} ions. This induces electron holes with a very high mobility in the t_2 (Co) band. Thus, the electronic conduction process for $x<0.9$ is due to the t_2–t_2 orbital overlapping leading to a very high electronic conductivity. If one assumes, as shown in Fig. 8, that the energy level of the Ni^{4+}/Ni^{3+} redox couple is very close to the t_2 (Co) band, at the $Li_{0.9}Ni_{0.1}Co_{0.9}O_2$ composition, the two transport mechanisms can occur simultaneously leading to the complex observed behaviour.

^{7}Li NMR study

As previously demonstrated, the static ^{7}Li NMR spectra of the $LiNi_{1-y}Co_yO_2$ solid solution samples may be separated into two components depending on the value of y.[18,28] The first signal (referred to as component I), which is strongly positively shifted and whose magnitude increases with increasing Ni^{3+} concentration, may be attributed to lithium ions interacting with at least one nickel ion as a first 3d neighbor (a Fermi contact shift results from the interaction of one localized single electron through the oxygen orbitals). The second narrower signal (component II) centred at δ 0 which is similar to that of $LiCoO_2$, corresponds to lithium surrounded only by diamagnetic cobalt ions as first 3d neighbors.

Fig. 9(*a*) shows the $LiNi_{0.1}Co_{0.9}O_2$ ^{7}Li NMR spectra resulting from the application of a static spin-echo sequence in the range 293–153 K. The spectrum recorded at 293 K

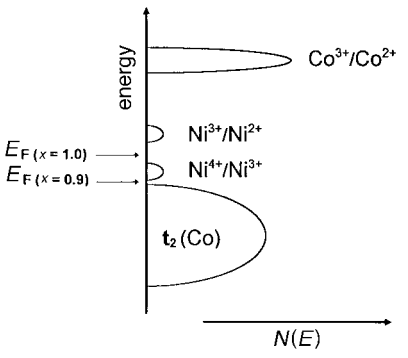

Fig. 8 Schematic representation of the band energy diagram showing the evolution of the Fermi level upon lithium deintercalation from the $LiNi_{0.1}Co_{0.9}O_2$ phase

shows the two components just discussed. Upon cooling, signal I broadens and shifts further owing to the increase of the magnetic susceptibility from the single electrons of Ni^{3+}. Signal II however is not affected by temperature, since it results from Li ions interacting only with diamagnetic Co^{3+} ions and since no mobility is involved.

After the galvanostatic extraction of 0.1 lithium ion (*i.e.* 0.1 electron), the NMR signal of the $Li_{0.9}Ni_{0.1}Co_{0.9}O_2$ electrode material was recorded at the same temperatures. As shown in Fig. 9(*b*), component I is no longer present even at low temperature, indicating the disappearance of magnetic Ni^{3+} ions. Besides, the NMR signal of $Li_{0.9}Ni_{0.1}Co_{0.9}O_2$ exhibits a symmetrical broadening upon cooling which results from a significant motional narrowing effect at room temperature. This is indeed a consequence of the lithium mobility within the interslab space since vacancies have been created by deintercalation.

When deintercalation is continued to $x=0.8$ (not shown in Fig. 9), a similar phenomenon is seen, but with a more significant motional narrowing. It is only for $x=0.7$ [Fig. 9(*c*)], that a new phenomenon appears, namely a slight global shift of the line towards the higher values of δ upon cooling. This is the consequence of the oxidation of some Co^{3+} ions to the tetravalent state, with the subsequent appearance of delocalized electrons as discussed above, and therefore of a Knight shift on the global NMR signal. Its changes with temperature are indeed less apparent than those observed in the case of the Fermi contact shift due to Ni^{3+} for $x=1.0$ since the latter applies only to some of the Li^+ ions (those which have a Ni^{3+} as a first cationic neighbour).

Fig. 10 shows static ^{7}Li NMR spectra of the deintercalated $Li_xNi_{0.1}Co_{0.9}O_2$ phases recorded at low temperature where mobility is minimized. The two redox processes, discussed above, are clearly apparent. From this figure, the $x=0.9$ composition seems not to exhibit any magnetic interaction. However, the electric measurements discussed above suggest

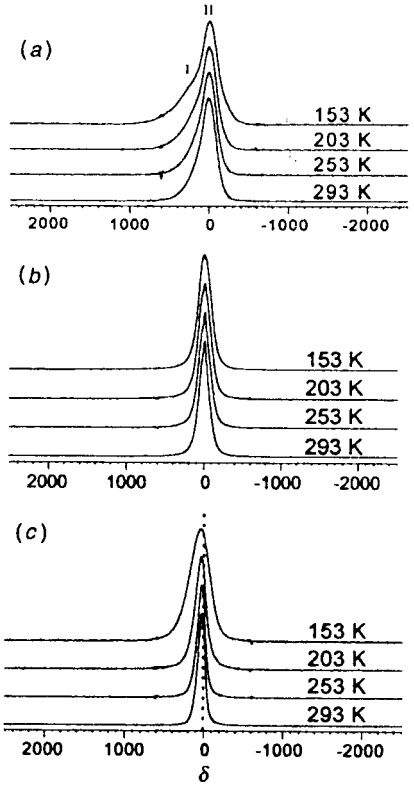

Fig. 9 Static ^{7}Li NMR spectra of the electrochemically deintercalated $Li_xNi_{0.1}Co_{0.9}O_2$ phases in the 293–153 K temperature range: (*a*) $LiNi_{0.1}Co_{0.9}O_2$ starting material, (*b*) $Li_{0.9}Ni_{0.1}Co_{0.9}O_2$ phase, (*c*) $Li_{0.7}Ni_{0.1}Co_{0.9}O_2$ phase

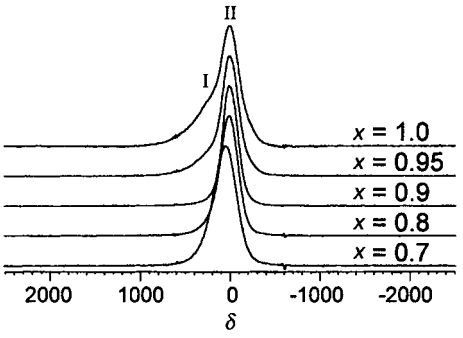

Fig. 10 Static low-temperature (153 K) ^{7}Li NMR spectra of the $Li_xNi_{0.1}Co_{0.9}O_2$ phases ($0.7 \leqslant x \leqslant 1$)

that some cobalt ions have already been oxidized at this composition; they must lead to too small a Knight shift for it to be detected by NMR spectroscopy under static conditions.

A similar NMR study has been performed for the $Li_xNi_{0.2}Co_{0.8}O_2$ system. Fig. 11 summarizes the results of the low-temperature NMR spectra of $Li_xNi_{0.2}Co_{0.8}O_2$ phases recorded with the same experimental conditions. A similar behaviour is observed. The broad shoulder (component I), which is indeed more prominent since there are twice as many Ni ions in the pristine phase, disappears gradually from $x=1.0$ to $x=0.8$ in relation to the oxidation of Ni^{3+} ions. The thermal variation of the NMR signal of the $Li_{0.8}Ni_{0.2}Co_{0.8}O_2$ composition (not reported here) indicates again that this phase exhibits only diamagnetic ions. For $x<0.7$, Knight shift behaviour is observed, corresponding to more delocalized electrons resulting from the Co^{3+} oxidation. Thus, the ^{7}Li NMR study fully confirms the preferential oxidation of Ni^{3+} as compared to Co^{3+} upon deintercalation.

General Discussion

All the results presented above show that the hypothesis of the selective oxidation of nickel before cobalt is a very general phenomenon in layered oxides. Indeed, this behaviour has been reported for $Na_xNi_{1-y}Co_yO_2$ oxides[23] and $H_xK_vNi_{1-y}Co_yO_2 \cdot zH_2O$ oxyhydroxides.[29] In both systems, only the nickel-rich materials were studied ($y \leqslant 0.5$) since the $NaNi_{1-y}Co_yO_2$ solid solution which is the parent of the two materials families, does not exist for $y>0.5$. One of the interests of the $Li_xNi_{1-y}Co_yO_2$ system is that it shows a solid solution for all nickel/cobalt ratios.

One interesting point to be discussed concerns the behaviour of the $Li_{0.9}Ni_{0.1}Co_{0.9}O_2$ phase for which a diamagnetic behaviour is expected in an ideal model. In fact, the transport properties study shows that a few cobalt ions are oxidized before the complete oxidation of all nickel ions. This result is emphasized by the shape of the electrochemical curve recorded at thermodynamic equilibrium (Fig. 3), which shows that the change in voltage associated with the change from one redox

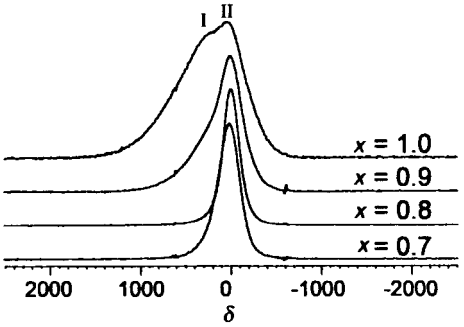

Fig. 11 Static low-temperature (153 K) ^{7}Li NMR spectra of the $Li_xNi_{0.2}Co_{0.8}O_2$ phases ($0.7 \leqslant x \leqslant 1$)

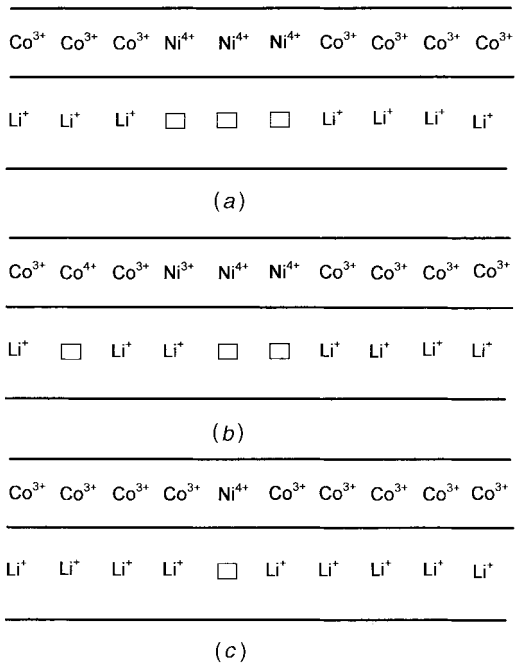

Fig. 12 Schematic representation of the relationship between the nickel/cobalt distributions within the $(Ni_{0.1}Co_{0.9}O_2)_n$ slab and the oxidation selectivity

system to the other occurs in a small domain and not for a fixed composition. One can assume that this behaviour must result from too small an energy difference between the Ni^{4+}/Ni^{3+} redox couple and the top of the t_2 (Co) band. One can also consider that the real distribution between nickel and cobalt ions within the slabs can have an effect on the selectivity of the oxidation process. As the Ni/Co ratio is quite low, a significant number of Ni^{3+} ions must have an environment (numbers of cobalt and nickel around them) different from the ideal statistical value. Indeed a tendency to a non-statistical Ni/Co distribution has been evidenced in the $LiNi_{1-y}Co_yO_2$ materials using ^7Li NMR spectroscopy.[28] Consider for example that a small cluster of nickel ions (three or four) exists within the slab, and that these ions are oxidized. In order to maintain the electrical neutrality at the local scale, the lithium vacancy resulting from the oxidation must stay in the vicinity of this cluster [Fig. 12(*a*)]. However, in the lithium plane, the electrostatic repulsions tend to distribute the mobile lithium statistically between all sites. Therefore, according to the relative energy difference between the two opposite effects, different behaviours can be expected: (*i*) preferential oxidation of nickel and existence of a lithium vacancy cluster associated with the nickel cluster in the slab [Fig. 12(*a*)], (*ii*) statistical distribution of lithium leading to oxidation of only some nickel ions of the clusters. In this case, some cobalt ions must be oxidized to preserve the short range electroneutrality [Fig. 12(*b*)]. In the case of an ideal distribution of nickel and cobalt, this competition between such opposite tendencies does not exist and nickel ions can be completely oxidized before oxidation of cobalt [Fig. 12(*c*)]. These hypotheses which do not question the preferential oxidation of nickel show that the local ionic distribution can play an important rôle as far as solid solutions are concerned.

Conclusion

Even though several studies have been made on the $LiNi_{1-y}Co_yO_2$ solid solution over the last decade, the literature gives only a few examples of articles concerning the evolution of the physical properties with the lithium content in $Li_xNi_{1-y}Co_yO_2$ phases. The rarity of such studies is probably related to the difficulty in preparing pure samples of these deintercalated phases by the usual chemical way. In this work, we have presented a soft chemistry route in order to elaborate selected $Li_xNi_{0.1}Co_{0.9}O_2$ phases by use of electrochemistry. A pelletized $LiNi_{0.1}Co_{0.9}O_2$ oxide has been used as the positive electrode material in the $Li//Li_xNi_{0.1}Co_{0.9}O_2$ electrochemical cell which is galvanostatically charged under low current density up to the desired $Li_xNi_{0.1}Co_{0.9}O_2$ composition. The homogeneity of the obtained phases, which is essential for the significance of the subsequent physical measurements, is controlled simultaneously by the steadiness of the open circuit voltage and is confirmed by X-ray diffraction. With this method, we have studied the changes of electronic transport properties and of the ^7Li NMR signal with the lithium content in the $Li_xNi_{0.1}Co_{0.9}O_2$ phases. These two sensitive techniques show clearly that Ni^{3+} ions are oxidized first to the tetravalent oxidation state. This selectivity in the oxidation reaction induces a break in the $V=f(x)$ cycling curve of the $Li//Li_xNi_{0.1}Co_{0.9}O_2$ cell around the composition $Li_{0.9}Ni_{0.1}Co_{0.9}O_2$. The X-ray diffraction study shows that no structural transformation occurs during the electrochemical cycling in the $(0.5 \leqslant x \leqslant 1.0)$ composition range.

The authors wish to thank J. P. Doumerc for fruitful discussion, E. Marquestaut and P. Dordor for the transport properties experiments and CNES for financial support.

References

1 K. Mizushima, P. C. Jones, P. J. Wiseman and J. B. Goodenough, *Mater. Res. Bull.*, 1980, **15**, 783.
2 T. Nagaura and K. Tozawa, *Prog Batteries Sol. Cells*, 1990, **9**, 209.
3 M. G. S. R. Thomas, W. I. F. David, J. B. Goodenough and P. Groves, *Mater. Res. Bull.*, 1985, **20**, 1137.
4 J. R. Dahn, U. von Sacken, M. W. Juzhow and H. Al Janabi, *J. Electrochem. Soc.*, 1991, **138**, 2.
5 T. Ohzuku, A. Ueda, M. Nagayama, Y. Iwakoshi and H. Komori, *Electrochim. Acta*, 1993, **38**, 1159.
6 M. Broussely, F. Perton, P. Biensan, J. M. Bodet, J. Labat, A. Lecerf, C. Delmas, A. Rougier and J. P. Pérès, *J. Power Sources*, 1995, **54**, 54.
7 A. Lecerf, M. Broussely and J. P. Gabano, *Eur. Pat. Appl.*, EP 89 110 158, 1989.
8 C. Delmas, I. Saadoune and A. Rougier, *J. Power Sources*, 1993, **43–44**, 595.
9 I. Saadoune and C. Delmas, *J. Mater. Chem.*, 1996, **6**, 193.
10 M. M. Thackeray, P. J. Johnson, L. A. de Picciotto, P. G. Bruce and J. B. Goodenough, *Mater. Res. Bull.*, 1984, **19**, 179.
11 J. M. Tarascon and D. Guyomard, *Electrochim. Acta*, 1993, **38**, 1221.
12 C. Delmas and I. Saadoune, *Solid State Ionics*, 1992, **53–56**, 370.
13 A. Rougier, I. Saadoune, P. Gravereau, P. Willmann and C. Delmas, *Solid State Ionics*, 1996, **90**, 83.
14 J. P. Pérès, C. Delmas, A. Rougier, M. Broussely, F. Perton, P. Biensan and P. Willmann, *J. Phys. Chem. Solids*, 1996, **57**, 1057.
15 R. J. Gummow and M. M. Thackeray, *J. Electrochem. Soc.*, 1993, **140**, 3365.
16 D. Gaurant, N. Baffier, B. Garcia and J. P. Pereira-Ramos, *Solid State Ionics*, 1996, **91**, 45.
17 I. Saadoune and C. Delmas, *J. Solid State Chem.*, in press.
18 M. Ménétrier, A. Rougier and C. Delmas, *Solid State Commun.*, 1994, **90**, 439.
19 P. Dordor, E. Marquestau and G. Villeneuve, *Rev. Phys. Appl.*, 1980, **15**, 1607.
20 M. G. S. R. Thomas, P. G. Bruce and J. B. Goodenough, *J. Electrochem. Soc.*, 1985, **132**, 1521.
21 W. Li, J. N. Reimers and J. R. Dahn, *Solid State Ionics*, 1993, **67**, 123.
22 J. M. Amatucci, J. M. Tarascon and L. C. Klein, *J. Electrochem. Soc.*, 1996, **143**, 1114.
23 I. Saadoune, A. Maazaz, M. Ménétrier and C. Delmas, *J. Solid State Chem.*, 1996, **122**, 111.

24 R. D. Shannon and C. T. Prewitt, *Acta Crystallogr., Sect. B*, 1969, **25**, 925.
25 J. B. Goodenough, *Prog. Solid State Chem.*, 1971, **5**, 279.
26 J. Molenda, A. Stoklosa and T. Bak, *Solid State Ionics*, 1989, **36**, 53.
27 C. Delmas, C. Faure and Y. Borthomieu, *Mater. Sci. Eng. B*, 1992, **13**, 89.
28 C. Marichal, J. Hirschinger, P. Granger, M. Ménétrier, A. Rougier and C. Delmas, *Inorg. Chem.*, 1995, **34**, 1773.
29 Y. Borthomieu, PhD Thesis, University of Bordeaux I, France, 1990.

Paper 7/03368K; *Received* 15*th May*, 1997